Coherent Ray-Space Hierarchy Via Ray Hashing and Sorting

Nuno T. Reis, Vasco S. Costa and João M. Pereira
INESC-ID / Instituto Superior Técnico, University of Lisbon, Rua Alves Redol 9, 1000-029 Lisboa, Portugal

Keywords: Rasterization, Ray-Tracing, Ray-Hashing, Ray-Sorting, Bounding-Cone, Bounding-Sphere, Hierarchies, GPU, GPGPU.

Abstract: We present an algorithm for creating an n-level Ray-Space Hierarchy (RSH) of coherent rays that runs on a GPU. Our algorithm uses a rasterization stage to process the primary rays, then inputs those results in the RSH stage which processes the secondary rays. The RSH algorithm generates bundles of rays, hashes them and sorts them. Thus we generate a ray list containing adjacent coherent rays to improve the rendering performance of the RSH vs a classical approach. Moreover, scene geometry is partitioned into a set of bounding spheres and, then, intersected with the RSH to further decrease the amount of false ray bundle-primitive intersection tests. We show that our technique notably reduces the amount of ray-primitive intersection tests, required to render an image. In particular it performs up to 50% better in this metric than other algorithms in this class.

1 INTRODUCTION

Naive Ray-Tracing (RT), algorithmic complexity is N x M where N rays are tested against M polygons. Performance is thus low, especially with complex scenes due to the amount of intersection tests. To optimize this naive approach, two common scene partition approaches, Object Hierarchies and Spatial Hierarchies, are followed to reduce the intersection tests. Our work instead focuses on Ray Hierarchy optimizations. This is a less well explored area of the RT domain and one that is complementary to the Object-Spatial Hierarchies. In particular, this paper presents the Coherent Ray-Space Hierarchy (CRSH) algorithm. CRSH builds upon the Ray-Space Hierarchy (RSH) (Roger et al., 2007) and Ray-Sorting algorithms (Garanzha and Loop, 2010). RSH uses a tree where each node stores a bounding sphere-cone containing a set of rays. The tree is built via a bottom-up procedure and traversed in a top-down fashion. Our CRSH algorithm adds Ray-Sorting to achieve higher efficiency in each tree node and then expands on this basis with mesh culling and improved hashing methods.

We hypothesize that improving the coherency of the rays within each tree node shall lead to tighter bounding sphere-cones, reducing the amount of intersections. We use hashing, tuned to the type of the ray (e.g. shadow, reflection and refraction), to improve hierarchy efficiency. Finally we introduce whole mesh bounding spheres to reduce intersection tests at the hierarchy top level. This shallow spherical BVH allows us to reduce ray-primitive intersections. We note that our technique uses a rasterization stage to compute primary rays, RT is reserved for secondaries.

Our main contributions are:

- a compact ray-space hierarchy (RSH) based on ray-indexing and ray-sorting to reduce the amount of ray-primitive intersections.
- improved hashing methods.
- culling meshes from the RSH prior to primitive traversal.

2 BACKGROUND AND RELATED WORK

Ray-tracing (Whitted, 1980) is a global illumination technique for synthesis of realistic images through recursive ray-casting. The ray tracing algorithm casts primary rays from the eye. When the rays intersect geometry they can generate extra secondary rays: e.g. shadow, reflection and refraction rays.

These rays differentiate ray-tracing from the rasterization algorithm as they allow realistic reflections, refractions and shadows without additional techniques. However at a cost making the ray-tracing approach compute expensive. There is extensive and ongoing research around its optimization. Much research involves hierarchies, in the Object or Spatial

T. Reis N., S. Costa V. and M. Pereira J.
Coherent Ray-Space Hierarchy Via Ray Hashing and Sorting.
DOI: 10.5220/0006098001950202
In *Proceedings of the 12th International Joint Conference on Computer Vision, Imaging and Computer Graphics Theory and Applications (VISIGRAPP 2017)*, pages 195-202
ISBN: 978-989-758-224-0

domains, to decrease intersection tests in a divide and conquer fashion.

Object and Spatial Hierarchies help accelerate intersection calculations by culling polygons and objects far from the rays, hence by reducing the amount geometry to test.

Ray-Space Hierarchies, use ray bundles or ray caching to achieve the goal of reducing intersections. Instead of creating hierarchies based on scene geometry, they are based on the rays being cast in each frame. Our work is based on this approach and employs ray bundling and ray hashing (Arvo and Kirk, 1987) (Aila and Karras, 2010).

Roger et al. (Roger et al., 2007)'s RSH algorithm has five steps. The scene is first rasterized, for the primary ray trace output, unlike in a traditional ray-tracer. The first batch of secondary rays is generated using this information and becomes the basis for the RSH. The secondaries are bundled into nodes with a sphere bounding ray origins and a cone bounding ray directions: this is the bottom-level of the tree. Upper levels are created by merging nodes from lower levels. Once the top-level is reached, the scene geometry is intersected with the RSH. Hits are stored as triangle-id/node-id integer pairs. Only these hits will be tested at the lower levels of the tree, reducing intersection tests within each level. However, since rays aren't sorted, even at lower levels of the tree, nodes will be quite wide requiring too much geometry intersections and increasing the amount of intersections. We attempt to solve this problem by sorting rays prior to creating the RSH.

Garanzha and Loop (Garanzha and Loop, 2010) introduced an algorithm using parallel primitives to adapt the ray-tracing algorithm to the GPU. Their algorithm sorts generated rays and creates tight-fit frustums on the GPU and then intersects them with the scene's Bounding Volume Hierarchy (BVH) tree built on the CPU. One of the most interesting aspects is the fast ray sorting step which is done with parallel GPU primitives. This reduces the overall time of the operation. This approach can be combined with Roger et al's (Roger et al., 2007) algorithm to create a more efficient RSH.

The DACRT (Mora, 2011) algorithm employs a ray-stream approach that generates a kd-tree on the fly, while traversing scene geometry, in order to achieve a low time to first image. Similarly to Roger's RSH it also uses conic packets to bundle secondary rays. However this procedure is limited by the fact that it can only bundle rays with the exact same origin within the same cone. In addition it ray-traces primary rays. This has additional computational overhead, compared to a rasterization mechanism, hence

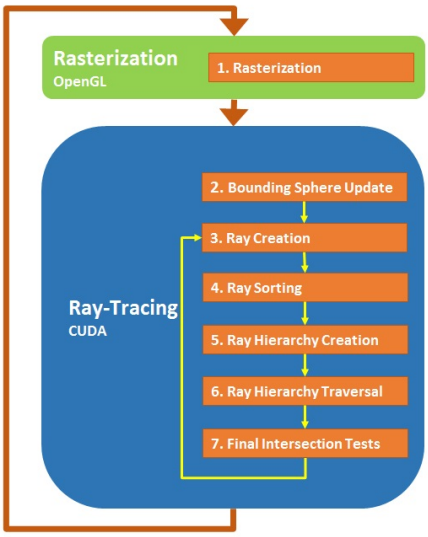

Figure 1: Coherent Ray-Space Hierarchy Overview.

it has worse rendering performance at primaries and less opportunities for bundling secondaries.

CHC+RT (Mattausch et al., 2015) uses combined hierarchies in ray space (RSH) and object space (BVH). It does not use explicit ray bounding primitives. It conservatively culls non-intersecting triangle and screen-space batches. This approach is more compute intensive on later stages due to the much simpler RSH, but results in less branch divergence, making it suitable for GPU implementation. The BVH is built offline, on the CPU, then transferred to the GPU. This high quality BVH has fast traversal time, for rapid rendering of static or rigid-body scenes, but the technique is poorly suited for dynamic geometry with a high time to first image.

3 OUR ALGORITHM

Our algorithm is performed in seven steps (see Figure 1). In each frame, steps 1 and 2 are executed just once while steps 3 through 7 are executed once per ray batch. Batches can have any combination of shadow, reflection, or refraction rays.

3.1 Rasterization

Rasterization is the first step to be performed. Although Rasterization solves the rendering problem conversely vs Ray-Tracing (i.e. projecting primitives to the screen, vs projecting rays backwards to the primitives), one can complement the other. The first set of rays, the primary rays, does not convey the global illumination effects that Ray-Tracing can

achieve, e.g. Shadows, Reflections and Refractions. Hence Rasterization can convey visual results similar to tracing primary rays, while being much faster and optimized in graphics hardware. Supplementing the Rasterization of primary rays with the Ray-Tracing of secondary rays get us the benefits from both techniques: the efficiency of Rasterization and the global illumination effects from Ray-Tracing.

In order to combine both techniques, the output from the fragment shaders used to rasterize the scene must provide more than just the fragment colors. We have to create different render targets according to the information we want to store. In our case, we output for each fragment its position and normal as well as its diffuse and specular properties. In terms of implementation, the fragment shader outputs four different textures, each containing four 32-bit floats per pixel. These textures are generated with OpenGL/GLSL and are then the first level of secondary rays are computed in CUDA.

3.2 Ray-Tracing

3.2.1 Bounding Sphere Update

Here we update object bounding spheres according to the transformations (e.g. translate, scale) applied to the object they contain. Since we only update the center and radius, there is no need to recalculate the bounding spheres in each frame (transformations do not invalidate bounding spheres). The minimum bounding sphere of the object meshes is precomputed with (Gärtner, 1999)s algorithm so there is no impact on render time performance.

3.2.2 Secondary Ray Creation

After the Rasterization step, we generate the secondary rays. We create an index, for each individual ray, to speed up ray sorting later on. We use a different hashing function for each type of ray (see Figures 2, 3). Since each ray has an origin and a direction it would be straightforward to use these parameters to create our hash. However for shadow rays it is sufficient to use the light-index, and the ray direction. This is doable if we invert the origin of the shadow ray so that it is located at the light source rather than the originating fragment. To reduce the size of the hash keys we convert the ray direction into spherical coordinates (Glassner, 1990) and store both, the light index and the spherical coordinates, into a 32-bit integer, with the light index having the higher bit-value such that the shadow rays are sorted a priori according to the light source.

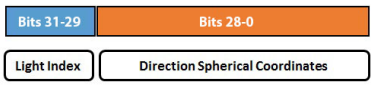

Figure 2: Shadow Ray Hash.

The Reflection and Refraction rays are also converted to spherical coordinates. However, in this case, the ray origin is used in the hash, given that these rays are not coherent with regards to the origin, unlike shadow rays.

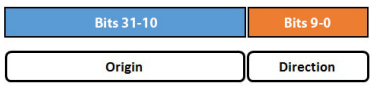

Figure 3: Reflection and Refraction Ray Hash.

Once generation is complete, we have an array with the generated secondary rays as well as two arrays with the ray keys (ray hashes) and the ray values (ray position in the ray array) and a final array with head flags which indicate if there is a ray in the corresponding position within the key-value arrays, where we store either a 0 or a 1, indicating if there is a ray or not, respectively. Using the information from the head flags array we then run a trimming operator on the key-value arrays (see Figure 4). This is done by first applying an inclusive scan operator (Merrill and Grimshaw, 2009) on the head flags array, which gives us the number of positions each pair needs to be shifted to the left. This is done in order to trim the arrays (Pharr and Fernando, 2005).

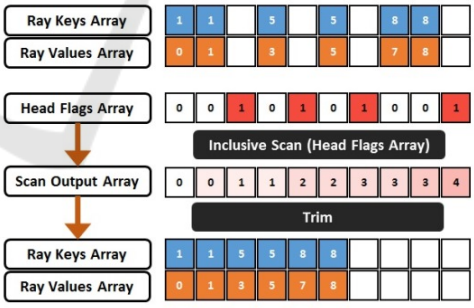

Figure 4: Array Trimming.

3.2.3 Secondary Ray Sorting

Here we use a compression-sorting-decompression scheme, expanding on prior work by Garanzha and Loops (Garanzha and Loop, 2010). The compression step exploits the local coherency of rays. Even for secondary rays, the bounces generated by two adjacent rays have a good chance of being coherent. This can result in the same hash value for both bounces. Given this information, we compress the ray key-value pairs into chunks, minimizing the number of

pairs that need to be sorted. To compress the pairs we utilize a head flags array with the same size as the key-value pair array, initializing it with 0s in every position and inserting 1s into positions in which the key (hash) of the corresponding pair differs from the previous pair. After populating the head flags array we apply an inclusive scan operator on it (Merrill and Grimshaw, 2009). By combining the head flags array with the scan output array we create the chunk keys, base and size arrays, which contain the hash, starting index and size of the corresponding chunks (see Figure 5). The chunk keys are represented in different colors at the image below. The chunk base array represents the original position of the first ray in the chunk while the chunk size array represents the size of the chunk, needed for the ray array decompression.

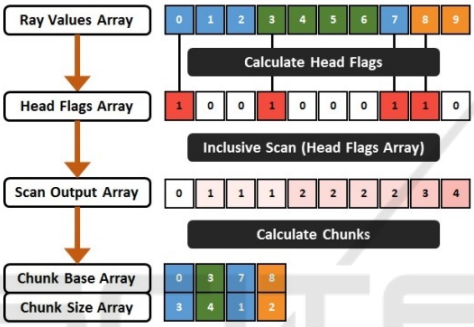

Figure 5: Ray Compression into Chunks.

After ray compression we have an array of chunks with the information required to reconstruct the initial rays array. So we can begin the actual sorting. We radix sort (Merrill and Grimshaw, 2010) the chunks array according to the chunk keys.

Decompression works by creating a skeleton array. This skeleton array is similar to the head flag arrays we created before except that it contains the size of the sorted chunks. Next we apply an exclusive scan operator on the skeleton array. This will give us the positions of the chunks starting positions on the sorted key and value arrays. After creating these two arrays for each position in the scan array we fill the sorted ray array. We start in the position indicated in the scan array and finish after filling the number of rays contained within the corresponding chunk.

3.2.4 Ray Hierarchy Creation

With the sorted rays we can now create the actual hierarchy. Since the rays are now sorted coherently the hierarchy will be much tighter in its lower levels, giving us a smaller number of intersection candidates as we traverse further down the hierarchy. Each node in the hierarchy is represented by a sphere and a cone

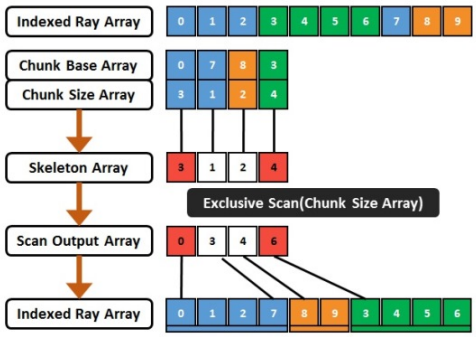

Figure 6: Ray Decompression from Chunks.

(see Figures 7, 8).

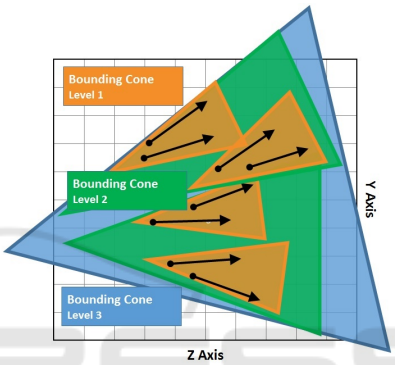

Figure 7: Bounding Cone - 2D View.

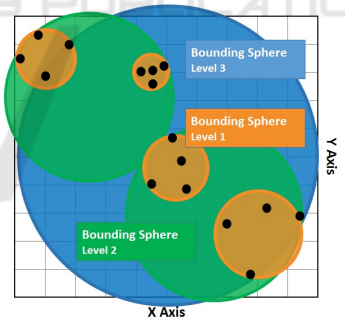

Figure 8: Bounding Sphere - 2D View.

The sphere contains all the nodes ray origins while the cone contain the rays themselves (see Figure 9). This structure is stored with eight floats: the sphere center and radius (four floats) and the cone direction and spread angle (four floats). Construction of the hierarchy is done in a bottom-up fashion. We start with the leaves, with spheres of radius 0 and a cone spread angle equal to 0. These leaves correspond to sorted rays. Parent nodes are created by merging child nodes. The number of children combined per node is parametrized.

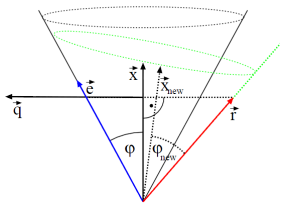

Figure 9: Cone-Ray Union - 2D View. courtesy of (Szécsi, 2006).

We use the formulas below to create compact cones (Szécsi, 2006) for the first level nodes.

$$\vec{q} = \frac{(\vec{x}\cdot\vec{r})\cdot\vec{x}-\vec{r}}{|(\vec{x}\cdot\vec{r})\cdot\vec{x}-\vec{r}|} \tag{1}$$

$$\vec{e} = \vec{x}\cdot\cos(\phi)+\vec{q}\cdot\sin\phi \tag{2}$$

$$\vec{x}_{new} = \frac{\vec{e}+\vec{r}}{|\vec{e}+\vec{r}|} \tag{3}$$

$$\cos\phi_{new} = \vec{x}_{new}\cdot\vec{r} \tag{4}$$

Otherwise we use these formulas to merge cones:

$$\vec{x}_{new} = \frac{\vec{x_1}+\vec{x_2}}{|\vec{x_1}+\vec{x_2}|} \tag{5}$$

$$\cos\phi_{new} = \frac{\arccos(\vec{x_1}+\vec{x_2})}{2}+\max(\phi_1,\phi_2) \tag{6}$$

Finally we merge spheres with this formula:

$$center_{new} = \frac{center_1+center_2}{2} \tag{7}$$

$$radius_{new} = \frac{|center_2-center_1|}{2}+\max(radius_1,radius_2) \tag{8}$$

Each ray needs to know the corresponding pixel. Rays are out of order due to sorting. We need a way to map rays back to screen pixels. Since the hierarchy is not tied to geometry in the scene it does not matter for hierarchy creation whether the scene is dynamic or static. What matters is the number of ray bounces, so if there are more pixels occupied in the screen, the hierarchy will have more nodes.

Roger et al. (Roger et al., 2007) also noted that some nodes might become too large as we travel higher up into the hierarchy. To mitigate this problem we decided to limit the number of levels generated and subsequently the number of levels traversed. Since rays are sorted before this step, there is much higher coherency between rays in the lower levels. If we focus on these rays and ignore the higher levels of the hierarchy we will have better results (as we shall see in Section 5). There is a possibility that we might end up having more local intersection tests but since the nodes in the higher levels of the hierarchy are quite large, we would most likely end up having intersections with every single triangle. Thus having no real gain from calculating intersections on these higher level nodes to begin with.

3.2.5 Ray Hierarchy Traversal

Once we have an hierarchy tree we can traverse it. Prior to traversal we compute the bounding spheres for each object in the scene using Bernd Gartners algorithm (Gärtner, 1999).

For the top level of the ray tree we intersect tree nodes with bounding spheres to further cull intersections. Finally we traverse the tree in a top-down order, intersecting each node with geometry. Since parent nodes fully contain child nodes, triangles rejected on parent nodes will not be tested again on child nodes. Let us say we start traversing the tree with the root node. If a triangle does not intersect the root then this means that specific triangle will not intersect any of the children. Since it is the root node, no ray in the scene will intersect it so we do not have to do any further intersections with it. We store the intersection information per level in an array so that child nodes know the sets of triangles they have to compute intersections against. The intersection tests being run at this stage are coarse grained. They use the triangle bounding spheres since we have to do the actual intersection tests in the final stage anyway. Intersection tests are run in parallel so there is an issue regarding empty spaces in the textures that contain intersection information. These arrays need to be trimmed using the same procedure that was used after ray generation. These hits are stored as an int32 in which the first 18 bits store the node id and the last 14 bits store the triangle id. This is not a problem for larger scenes as those are processed in triangle batches. Each hit only needs to store the maximum number of triangles per batch.

To calculate the intersection with the node, i.e. the union of a sphere and a cone, we simplify the problem by enlarging the triangles bounding sphere (Ericson, 2004) and reducing the cones size (see Figure 10). Cone-sphere intersections were described by Amanatides (Amanatides, 1984). We use the formula in Roger et al. (Roger et al., 2007).

$$result = |C-H|\times\tan\alpha+\frac{d+r}{\cos\alpha} \geqslant |P-H| \tag{9}$$

Table 1: OFFICE (251.55 K shadow rays), CORNELL (184.72 K shadow & 524.29 K reflection rays), SPONZA (256.71 K shadow rays) global rendering performance.

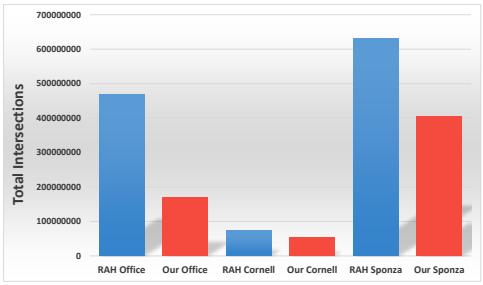

	OFFICE		CORNELL		SPONZA	
ALGORITHM	TOTAL # ISECT	RELATIVE %	TOTAL # ISECT	RELATIVE %	TOTAL # ISECT	RELATIVE %
Brute Force	9133.13 M	100%	606.91 M	100%	17058.58 M	100%
RAH Algorithm	469.68 M	5.14%	72.87 M	12.01%	632.41 M	3.71%
Our Algorithm	**170.07 M**	**1.86%**	**53.58 M**	**8.83%**	**405.62 M**	**2.38%**

Table 2: OFFICE, CORNELL, SPONZA rendering details.

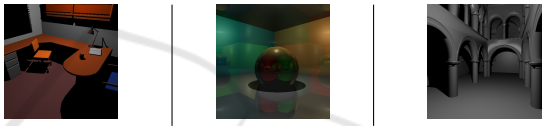

	OFFICE		CORNELL		SPONZA	
	LEVEL 2	LEVEL 1	LEVEL 2	LEVEL 1	LEVEL 2	LEVEL 1
RAH Algorithm						
# SH INTERSECTIONS	142.73 M	202.03 M	3.00 M	5.17 M	266.60 M	261.49 M
# SH MISSES	117.47 M	186.41 M	2.35 M	3.61 M	233.91 M	248.46 M
# SH HITS	25.25 M	15.62 M	0.65 M	1.56 M	32.69 M	13.04 M
# RE INTERSECTIONS			6.49 M	17.80 M		
# RE MISSES			4.26 M	14.31 M		
# RE HITS			2.23 M	3.49 M		
Our Algorithm						
# SH INTERSECTIONS	11.56 M	85.57 M	0.75 M	2.38 M	266.60 M	62.67 M
# SH MISSES	0.86 M	76.46 M	0.45 M	0.98 M	258.76 M	53.12 M
# SH HITS	10.70 M	9.12 M	0.30 M	1.40 M	7.83 M	9.55 M
# RE INTERSECTIONS			2.74 M	10.27 M		
# RE MISSES			1.45 M	6.98 M		
# RE HITS			1.28 M	3.29 M		

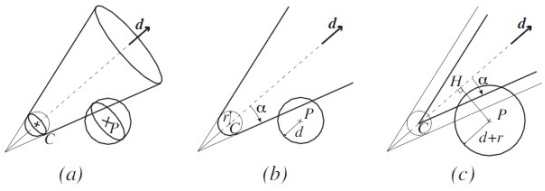

Figure 10: Cone-Ray Union - 2D View. courtesy of (Roger et al., 2007).

3.2.6 Final Intersection Tests

After traversing the hierarchy we have an array of node id and triangle id pairs which represent candidates for the local intersection tests (Möller, 1997). In this final step all that remains is to find out which is the closest intersected triangle for each ray and accumulate shading. Depending on the depth that we want for the algorithm we might need to output another set of secondary rays. Since the algorithm is generic, all that is necessary for this is to output these rays onto the ray array that we used initially and continue from the ray-sorting step.

4 TEST METHODOLOGY

We implemented our CRSH algorithm in OpenGL/C++ and CUDA/C++ and then compared it with our implementation of RAH (Roger et al., 2007) over the same architecture. We map our algorithm onto the GPU, fully parallelizing it

there. We achieve this mainly by the use of parallel primitives, like prefix sums (Blelloch, 1990). We used the CUB (Merrill and Grimshaw, 2009; Merrill and Grimshaw, 2010) library to perform parallel radix sorts and prefix sums.

We measure the amount of intersections, including misses and hits, to evaluate ray hierarchy algorithms proficiency at reducing the amount of ray-primitive intersection tests required to render an image. All scenes were rendered at 512×512 resolution using an hierarchy depth of 2 and a node subdivision of 8 (each upper level node in the hierarchy consists of the combination of 8 nodes from the level directly below).

The test information was collected using a NVIDIA GeForce GTX 770M GPU with 3 GB of RAM. Our algorithm is completely executed on the GPU (including hierarchy construction and traversal) so the CPU has no impact on the test results.

We used three different scenes, OFFICE, CORNELL and SPONZA.

The OFFICE scene (36K triangles) is representative of interior design applications. It is divided into several sub-meshes; therefore it adapts very well to our bounding volume scheme. For this scene the emphasis was on testing shadow rays.

We selected CORNELL (790 triangles). as it is representative of highly reflective scenes. It consists an object surrounded by six mirrors. On this scene we focused on testing reflection rays although it also features shadow rays in it.

SPONZA (66K triangles), much like OFFICE, is representative of architectural scenes. For this scene the emphasis was also on testing shadow rays but for scenes that do not conform with our bounding volume scheme. This scene does not adapt well to our scheme as is not divided into submeshes.

5 RESULTS AND DISCUSSION

5.1 Intersection Results

We hypothesised that our more coherent RSH needs to compute fewer intersections to render a scene. We expect more expressive results for shadow rays. As shadow rays have low divergence classification should be more coherent than for reflection rays. Additionally our hierarchy should be more coherent with reflection rays than one based on RAH due to the hashing used. However the incoherence of reflection rays, vs shadow rays, should lead to a lower quality hierarchy.

Our initial expectations for Office were to get a much lower number of intersection tests with our algorithm than with RAH. The scene is a good fit to our bounding volume scheme and our highly coherent shadow ray hierarchy. Results (see Table 2) confirm our initial expectations: we compute 63.79% less intersections than RAH on this scene. 98.14% less than a brute force approach.

The Cornell scene has reflection rays, which are more incoherent, so we expected worse results than with Office. Still we compute 26.47% less intersections (shadow and reflection rays combined) than the RAH algorithm and 91.17% less than the brute force approach.

The final scene, Sponza, is a whole mesh. We did not employ object subdivision in this scene. Hence we expected worse results than with Office since we would only get the benefit of the shadow ray hierarchy and none from the bounding volume scheme.

We compute 35.86% less intersections than RAH and 97.62% less than brute force. Since there is no mesh culling for this scene the results are not as good as with Office but we still manage to outperform RAH even without using an integral part of our algorithm.

5.2 Performance Results

These tests were run over the course of 58 frames and the results for each phase are the average of these 58 frames.

The major time consuming steps are hierarchy traversal and final intersections. The biggest advantage between our algorithm and the RAH algorithm resides in the time spent traversing the hierarchy. Our algorithm is 2.18x faster at traversal than RAH in Office (see Table 3). This increased time spent traversing the hierarchy means RAH takes about 100% more time to render each frame than our algorithm.

Table 3: OFFICE, CORNELL, SPONZA render times.

	OFFICE	CORNELL	SPONZA
RAH	TIME (MS)	TIME (MS)	TIME (MS)
RAY CREATION	40.24	125.73	41.22
RAY COMPRESSION	0.00	0.00	0.00
RAY SORTING	0.00	0.00	0.00
RAY DECOMPRESSION	0.00	0.00	0.00
HIERARCHY CREATION	122.17	366.99	126.50
Ours	TIME (MS)	TIME (MS)	TIME (MS)
RAY CREATION	40.43	128.13	41.50
RAY COMPRESSION	16.65	53.92	17.15
RAY SORTING	11.82	50.97	12.70
RAY DECOMPRESSION	99.72	251.95	98.62
HIERARCHY CREATION	130.63	407.09	137.84
Ours vs RAH	SPEEDUP	SPEEDUP	SPEEDUP
HIERARCHY TRAVERSAL	2.18X	1.53X	1.06X
FINAL INTERSECTION TESTS	1.32X	1.02X	1.14X

Much like Office, the Cornell scene takes most of its time on traversal and calculating the final intersec-

tions. However due to the lower geometric complexity the absolute values aren't as high. Our algorithm performs traversal 1.53x faster than RAH in Cornell, a significant reduction.

Finally for the Sponza scene we see a similar relative time spent in the traversal of the hierarchy vs previous scenes. Even though the Sponza scene isn't subdivided into separate object meshes, we manage to slightly outperform RAH at traversal.

6 CONCLUSIONS AND FUTURE WORK

Our paper described an algorithm to create a Ray-Space Hierarchy which markedly reduces the intersections, required to ray-trace a scene, due to improved coherency and a shallow BVH.

We achieved our goal of reducing intersections using a Ray-Space Hierarchy. This technique is orthogonal to the use of both Object and Space Hierarchies. These can be used together to obtain even better results. Our results show a reduction in computed intersections of 50% for shadow rays and 25% for reflection rays compared to previous state of the art RSHs.

There is room for improvements: Since the hash determines how rays are sorted, an hierarchy will improve if we enhance the ray spatial coherency. We used spherical bounding volumes and a shallow BVH. In the future we aim to combine our coherent ray hierarchy with a deeper BVH to further descrease ray-primitive intersections e.g. (Bradshaw and O'Sullivan, 2004).

ACKNOWLEDGEMENTS

This work was supported by national funds through Fundação para a Ciência e Tecnologia (FCT) with reference UID/CEC/50021/2013.

REFERENCES

Aila, T. and Karras, T. (2010). Architecture Considerations for Tracing Incoherent Rays. In *Proceedings of the Conference on High Performance Graphics*, pages 113–122. Eurographics Association.

Amanatides, J. (1984). Ray Tracing with Cones. *SIGGRAPH Computer Graphics*, 18(3):129–135.

Arvo, J. and Kirk, D. (1987). Fast Ray Tracing by Ray Classification. *SIGGRAPH Computer Graphics*, 21(4):55–64.

Blelloch, G. E. (1990). Prefix Sums and their Applications. Technical report, Carnegie Mellon University.

Bradshaw, G. and O'Sullivan, C. (2004). Adaptive Medial-Axis Approximation for Sphere-tree Construction. *ACM Transactions on Graphics (TOG)*, 23(1):1–26.

Ericson, C. (2004). *Real-Time Collision Detection*. Series in Interactive 3-D Technology. Morgan Kaufmann Publishers Inc.

Garanzha, K. and Loop, C. (2010). Fast Ray Sorting and Breadth-First Packet Traversal for GPU Ray Tracing. *Computer Graphics Forum*, 29(2):289–298.

Gärtner, B. (1999). Fast and Robust Smallest Enclosing Balls. In *Proceedings of the 7th Annual European Symposium on Algorithms*, ESA '99, pages 325–338. Springer-Verlag.

Glassner, A. S., editor (1990). *Graphics Gems*. Academic Press, Inc.

Mattausch, O., Bittner, J., Jaspe, A., Gobbetti, E., Wimmer, M., and Pajarola, R. (2015). CHC+RT: Coherent Hierarchical Culling for Ray Tracing. *Computer Graphics Forum*, 34(2):537–548.

Merrill, D. and Grimshaw, A. (2009). Parallel Scan for Stream Architectures. Technical report, University of Virginia, Department of Computer Science.

Merrill, D. G. and Grimshaw, A. S. (2010). Revisiting Sorting for GPGPU Stream Architectures. In *Proceedings of the 19th International Conference on Parallel Architectures and Compilation Techniques*, PACT '10, pages 545–546. ACM.

Möller, T. (1997). A Fast Triangle-Triangle Intersection Test. *Journal of Graphic Tools*, 2(2):25–30.

Mora, B. (2011). Naive Ray-Tracing: A Divide-And-Conquer Approach. *ACM Transactions on Graphics (TOG)*, 30(5):117.

Pharr, M. and Fernando, R. (2005). *GPU Gems 2: Programming Techniques for High-Performance Graphics and General-Purpose Computation*. GPU Gems. Addison-Wesley Professional.

Roger, D., Assarsson, U., and Holzschuch, N. (2007). Whitted Ray-tracing for Dynamic Scenes Using a Ray-space Hierarchy on the GPU. In *Proceedings of the 18th Eurographics Conference on Rendering Techniques*, EGSR '07, pages 99–110. Eurographics Association.

Szécsi, L. (2006). The Hierarchical Ray Engine. In *WSCG Full Papers Proceedings*, pages 249–256. Václav Skala-UNION Agency.

Whitted, T. (1980). An Improved Illumination Model for Shaded Display. *Commun. ACM*, 23(6):343–349.